THE JOURNAL OF BIOLOGICAL CHEMISTRY VOL. 283, NO. 50, pp. 34819–34832, December 12, 2008

Calcium-independent Phospholipase A_2 (iPLA$_2\beta$)-mediated Ceramide Generation Plays a Key Role in the Cross-talk between the Endoplasmic Reticulum (ER) and Mitochondria during ER Stress-induced Insulin-secreting Cell Apoptosis*

Received for publication, September 24, 2008, and in revised form, October 15, 2008 Published, JBC Papers in Press, October 20, 2008, DOI 10.1074/jbc.M807409200

Xiaoyong Lei, Sheng Zhang, Alan Bohrer, and Sasanka Ramanadham[1]

From the Department of Medicine, Mass Spectrometry Resource and Division of Endocrinology, Metabolism, and Lipid Research, Washington University School of Medicine, St. Louis, Missouri 63110

Endoplasmic reticulum (ER) stress induces INS-1 cell apoptosis by a pathway involving Ca^{2+}-independent phospholipase A_2 (iPLA$_2\beta$)-mediated ceramide generation, but the mechanism by which iPLA$_2\beta$ and ceramides contribute to apoptosis is not well understood. We report here that both caspase-12 and caspase-3 are activated in INS-1 cells following induction of ER stress with thapsigargin, but only caspase-3 cleavage is amplified in iPLA$_2\beta$ overexpressing INS-1 cells (OE), relative to empty vector-transfected cells, and is suppressed by iPLA$_2\beta$ inhibition. ER stress also led to the release of cytochrome *c* and Smac and, unexpectedly, their accumulation in the cytosol is amplified in OE cells. These findings raise the likelihood that iPLA$_2\beta$ participates in ER stress-induced apoptosis by activating the intrinsic apoptotic pathway. Consistent with this possibility, we find that ER stress promotes iPLA$_2\beta$ accumulation in the mitochondria, opening of mitochondrial permeability transition pore, and loss in mitochondrial membrane potential ($\Delta\Psi$) in INS-1 cells and that these changes are amplified in OE cells. ER stress also led to greater ceramide generation in ER and mitochondria fractions of OE cells. Exposure to ceramide alone induces loss in $\Delta\Psi$ and apoptosis and these are suppressed by forskolin. ER stress-induced mitochondrial dysfunction and apoptosis are also inhibited by forskolin, as well as by inactivation of iPLA$_2\beta$ or NSMase, suggesting that iPLA$_2\beta$-mediated generation of ceramides via sphingomyelin hydrolysis during ER stress affect the mitochondria. In support, inhibition of iPLA$_2\beta$ or NSMase prevents cytochrome *c* release. Collectively, our findings indicate that the iPLA$_2\beta$-ceramide axis plays a critical role in activating the mitochondrial apoptotic pathway in insulin-secreting cells during ER stress.

Diabetes mellitus is the most prevalent human metabolic disease resulting from the loss and/or dysfunction of β-cells in pancreatic islets. Type 1 diabetes mellitus (T1DM)[2] is caused by autoimmune β-cell destruction (1) and apoptosis plays a prominent role in the loss of β-cells during development of T1DM (1, 2). Type 2 diabetes mellitus (T2DM) results from a progressive decline in β-cell function and chronic insulin resistance (3, 4) that is also associated with decreases in β-cell mass due to increased β-cell apoptosis (5, 6).

Autopsy studies indicate that the β-cell mass in obese T2DM subjects is smaller than that in obese non-diabetic subjects (7, 8) and that the loss in β-cell function in non-obese T2DM is associated with decreases in β-cell mass (5, 6). β-Cell mass is regulated by a balance between β-cell replication/neogenesis and β-cell death resulting from apoptosis (9, 10). Findings in rodent models of T2DM (10, 11) and in human T2DM (5, 6) indicate that the decrease in β-cell mass in T2DM is not attributable to reduced β-cell proliferation or neogenesis but to increased β-cell apoptosis. Emerging evidence also suggests that cytokine-mediated β-cell apoptosis is a contributor to β-cell death during the development of autoimmune T1DM (1, 2, 12, 13). It is therefore important to understand the mechanisms underlying β-cell apoptosis if this process is to be prevented or delayed.

β-Cell apoptosis can be mediated via an extrinsic pathway involving interaction of a stimulant with death receptors residing in the plasma membrane or via an intrinsic pathway involving mitochondrial signaling (14). A third organelle gaining prominence as a participant in apoptosis is the endoplasmic reticulum (ER) (14, 15). A number of factors can induce ER stress leading to the onset of various diseases, including Alzheimer and Parkinson (16). β-Cell death in the Akita diabetic (17, 18) and NOD.k iHEL nonimmune (19) diabetic mouse models is also attributed to ER stress. In addition, mutations in genes encoding the ER-stress transducing enzyme pancreatic ER kinase (PERK) (20) and the ER resident protein involved in degradation of malfolded ER proteins have been clinically linked to diminished β-cell health (21, 22). Several recent reports suggest

* This work was supported, in whole or in part, by National Institutes of Health Grants R01-DK69455, R37-DK34388, P41-RR00954, P60-DK20579, and P30-DK56341. The costs of publication of this article were defrayed in part by the payment of page charges. This article must therefore be hereby marked "*advertisement*" in accordance with 18 U.S.C. Section 1734 solely to indicate this fact.

[1] To whom correspondence should be addressed: Campus Box 8127, 660 S. Euclid Ave., St. Louis, MO 63110. Tel.: 314-362-8194; Fax: 314-362-7641; E-mail: sramanad@dom.wustl.edu.

[2] The abbreviations used are: T1DM, type 1 diabetes mellitus; T2DM, type 2 diabetes mellitus; BEL, bromoenol lactone suicide inhibitor of iPLA$_2\beta$; CM, ceramide; ECL, enhanced chemiluminescence; ER, endoplasmic reticulum; GPC, glycerophosphocholine; iPLA$_2\beta$, β-isoform of group VIA calcium-independent phospholipase A_2; ESI, electrospray ionization; $\Delta\Psi$, mitochondrial membrane potential; MS, mass spectrometry; PTP, mitochondrial permeability transition pore; NSMase, neutral sphingomyelinase; OE, iPLA$_2\beta$-overexpressing INS-1 cells; PBS, phosphate-buffered saline; PLA_2, phospholipase A_2; SM, sphingomyelin; TUNEL, terminal deoxynucleotidyl transferase-mediated (fluorescein) dUTP nick end labeling; DMSO, dimethyl sulfoxide; PERK, pancreatic ER kinase; eIF, eukaryotic initiation factor; DAPI, 4′,6-diamidino-2-phenylindole.

that ER stress can play a prominent role in the autoimmune destruction of β-cells during the development of T1DM (13, 23, 24). Because the secretory function of β-cells endows them with a highly developed ER and the β-cell is one of the most sensitive cells to nitric oxide (25), it is not unexpected that β-cells exhibit a heightened susceptibility to autoimmune-mediated ER stress (26, 27). In support of this, Wolfram syndrome, which is associated with juvenile-onset diabetes mellitus, is recognized to be a consequence of chronic ER stress in pancreatic β-cells (23, 28).

In addition to serving as a cellular Ca^{2+} store, the ER is the site of secretory protein synthesis, assembly, folding, and post-translationally modification. Interruption of any of these functions can lead to production of malfolded mutant proteins that require rapid degradation. When an imbalance between the load of client proteins on the ER and the ability of the ER to process the load occurs, ER stress results (29). Prolonged ER stress promotes induction of stress factors and activation of caspase-12, localized to the ER (15), and can subsequently lead to downstream activation of caspase-3, a protease recognized to be the executioner of apoptosis (30). Being a site for Ca^{2+} storage, the ER responds to various stimuli to release Ca^{2+} and is therefore extremely sensitive to changes in cellular homeostasis. Although ER stress alone can induce the necessary factors to cause apoptosis, it is becoming increasingly apparent that the mitochondria, as an organelle that sequesters Ca^{2+} released from the ER, plays an important role in supporting the apoptosis process initiated by ER stress (31, 32).

Thapsigargin, which depletes ER Ca^{2+} stores by inhibiting sarcoendoplasmic reticulum Ca^{2+}-ATPase, causes ER stress in pancreatic islets and promotes hydrolysis of arachidonic acid. Surprisingly, the accumulation in arachidonic acid is suppressed by a bromoenol lactone (BEL) suicide-substrate inhibitor of Ca^{2+}-independent phospholipase A_2 (iPLA$_2\beta$) (33). These observations raise the possibility that iPLA$_2\beta$ participates in ER stress in β-cells. In support of this, ER stress-induced INS-1 cell apoptosis is amplified in iPLA$_2\beta$ overexpressing cells and is suppressed by BEL (34, 35).

The PLA$_2$s are a diverse group of enzymes that catalyze hydrolysis of the *sn*-2 substituent from glycerophospholipid substrates to yield a free fatty acid and a 2-lysophospholipid (36). Among the recognized PLA$_2$s is one that does not require Ca^{2+} for activity and is classified as a Group VIA iPLA$_2$ and is designated as the β-isoform of iPLA$_2$ (iPLA$_2\beta$) (37). The iPLA$_2\beta$ enzyme is activated by ATP and is inhibited by BEL (38). In addition to its proposed roles in phospholipid remodeling and signal transduction (39), iPLA$_2\beta$ contributes to apoptosis in many cell types, including β-cells (34, 35, 40). However, the mechanism by which iPLA$_2\beta$ activation contributes to apoptotic cell death has not yet been elucidated.

Pancreatic islet β-cells and insulinoma cells express iPLA$_2\beta$ activity that is sensitive to inhibition by BEL (41) and recent reports demonstrate that induction of ER stress promotes ceramide accumulations in INS-1 cells that can be attenuated by inactivation of iPLA$_2\beta$ (34, 35). Ceramides are complex lipids that can suppress cell growth and induce apoptosis (42, 43) and various reports (31, 44) suggest that ceramides can also disturb mitochondrial homeostasis. Here, we present evidence for the involvement of iPLA$_2\beta$-mediated ceramide generation in activating the mitochondrial apoptotic pathway during ER stress-induced insulin-secreting cell death.

EXPERIMENTAL PROCEDURES

Materials—The sources for the material used were as follows: (16:0/[^{14}C]-18:2)-GPC (PLPC, 55 mCi/mmol), rainbow molecular mass standards, and enhanced chemiluminescence (ECL) reagent, Amersham Biosciences; ceramide and other lipid standards, Avanti Polar Lipids, Alabaster, AL; Coomassie reagent, SDS-PAGE supplies and Triton X-100, Bio-Rad; mitochondrial membrane potential detection kit, Cell Technology Inc., Mountain View, CA; paraformaldehyde, Electron Microscopy Sciences, Ft. Washington, PA; forskolin, EMD Biosciences, San Diego, CA; normal goat serum, Cy3-conjugated affinipure goat anti-rabbit IgG (H+L), Jackson ImmunoResearch Laboratories, West Grove, PA; pentex fraction V fatty acid-free bovine serum albumin, Miles Laboratories, Eckert, IN; mitoprobe transition pore assay kit, Slow Fade® light antifade kit, Molecular Probes, Eugene, OR; peroxidase-conjugated goat anti-rabbit IgG antibody, TUNEL kit, Roche Diagnostic Corporation; primary antibodies, Santa Cruz Biotechnology. Inc., Santa Cruz, CA; and C2-ceramide, protease inhibitor mixture, thapsigargin, common reagents, and salts, Sigma.

Preparation, Culture, and Treatment of Stably Transfected INS-1 Cells—Control (empty-vector transfected) and iPLA$_2\beta$ overexpressing INS-1 cells were generated and cultured, as described (34). The cells were grown to confluence in cell culture Petri dishes or flasks and treated with vehicle (DMSO, 0.50 μl/ml), thapsigargin (1 μM), or C2-ceramide (C2-CM, 50 μM). To examine the effects of inhibiting iPLA$_2\beta$ activity, BEL (1 μM) was added to cells for 1 h and the medium was replaced with one containing DMSO or thapsigargin. The effects of elevating intracellular cAMP concentrations or inhibiting neutral sphingomyelinase were examined by treating the cells for 1 h with forskolin (2.5 μM) or GW4869 (10 μM), respectively, prior to addition of DMSO, thapsigargin, or C2-CM. All incubations were done at 37 °C under an atmosphere of 95% air, 5% CO_2.

In Situ Detection of DNA Cleavage by TUNEL and DAPI Staining—At the end of a treatment protocol, INS-1 cells were harvested and washed twice with ice-cold PBS. The cells were then immobilized on slides by cytospin (35) and fixed with 4% paraformaldehyde (in PBS, pH 7.4, 1 h, room temperature). The cells were then washed with PBS, and incubated in permeabilization solution (0.1% Triton-X-100 in 0.1% sodium citrate, PBS, 30 min, room temperature). The permeabilization solution was then removed and the TUNEL reaction mixture (50 μl) was added and the cells were incubated (1 h, 37 °C) in a humidified chamber. The cells were washed again with PBS and counterstained with DAPI (1 μg/ml) in PBS for 10 min to identify cellular nuclei. The incidence of apoptosis was assessed under a fluorescence microscope (Nikon Eclipse TE300) using a fluorescein isothiocyanate filter. Cells with TUNEL-positive nuclei were considered apoptotic. DAPI staining was used to determine the total number of cells in a field. A minimum of three fields per slide was used to calculate percent of apoptotic cells.

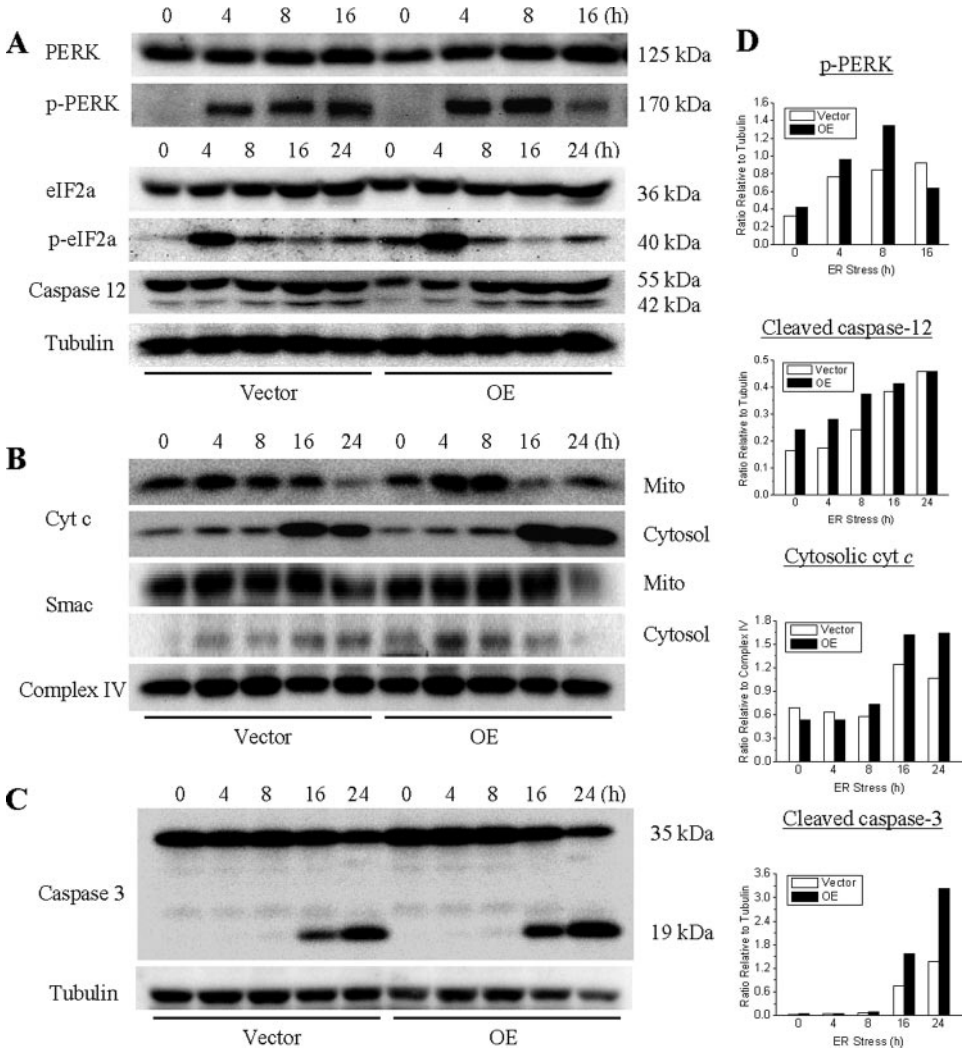

FIGURE 1. **ER stress-induced expression of ER- and mitochondria-related factors.** INS-1 cells were treated with either vehicle (*DMSO*) or thapsigargin (1 μM) and incubated for up to 24 h. At various times, the cells were harvested and cytosol and mitochondrial fractions were prepared. Proteins in each fraction were then resolved by SDS-PAGE and processed for immunoblotting analyses. Tubulin or complex IV immunoreactivity was used as control. *A*, ER factors. *B*, mitochondrial factors. *C*, caspase-3. Immunoreactive bands were visualized by ECL. *D*, quantitation of band intensities. Ratios of factor to control band intensity from a representative blot are presented (Vector, empty vector-transfected and OE, iPLA$_2\beta$-overexpressing INS-1 cells). Each analysis was done three times.

Assessment of Mitochondrial Membrane Potential ($\Delta\Psi$) by Flow Cytometry—Loss of $\Delta\Psi$ is an important step in the induction of cellular apoptosis (46). INS-1 cell $\Delta\Psi$ was therefore measured using a commercial kit according to the manufacturer's instructions. Briefly, harvested cells were washed once with PBS and resuspended in 100 μl of PBS ($\sim 1 \times 10^5$ cells/ml). An aliquot (5 μl) of Mito Flow fluorescent reagent was then added and the cell suspension was incubated at 37 °C for 30 min. The cells were then transferred to appropriate fluorescence-activated cell sorting tubes and diluted 1:5 with buffer provided in the kit. Fluorescence in cells was analyzed by flow cytometry (BD Biosciences) at an excitation wavelength of 488 nm.

Mitochondrial Permeability Transition Pore (PTP)—The PTP opening was measured in intact INS-1 cells by monitoring calcein-AM fluorescence in the absence and presence of $CoCl_2$, which quenches cytosolic fluorescence, as described (47). Briefly, INS-1 cells were washed twice with PBS and resuspended (1×10^6 cells/ml) in pre-warmed Hanks' balanced salt solution containing 2 mM Ca^{2+}. The cells were then loaded with calcein-AM for 15 min at 37 °C according to the manufacturer's instructions (Molecular Probes). In parallel experiments, similar cell samples were loaded with calcein-AM in the presence of $CoCl_2$. After washing away excess stain and quenching reagent, the cell pellets were resuspended in 400 μl of Hanks' balanced salt solution containing Ca^{2+} and analyzed for calcein-AM fluorescence by flow cytometry using a BD Biosciences FACscan flow cytometer in conjunction with WinMDI 2.8 software (excitation/emission, 494/517 nm).

Cell Fractionation—Cells were harvested and washed twice (750 $\times$ *g*, 5 min, 4 °C) with 10 volumes of ice-cold PBS. The cell pellet was suspended in 3 volumes of ice-cold isolation buffer (20 mM HEPES-KOH, pH 7.8, 250 mM sucrose, 1 mM EGTA, 10 mM potassium chloride), supplemented with protease inhibitor mixture (50 μl/ml). The cells were placed on ice for 15 min and then transferred to a Dounce homogenizer (Kimble/Kontes, Vineland, NJ) and disrupted by douncing 15 times on ice. The homogenate was centrifuged at 800 $\times$ *g* for 5 min to remove unbroken cells and nuclei, and the supernatant was then re-centrifuged (10,000 $\times$ *g*, 15 min, 4 °C) to obtain mitochondria. The supernatant was further subjected to ultracentrifugation (100,000 $\times$ *g*, 60 min, 4 °C). The resultant supernatant was the cytosolic fraction and the pellet contained ER. Plasma membrane fraction was prepared as described (48). Purity of the cellular fractions was verified by the 5′-nucleotidase (plasma membrane enzyme) activity assay and immunoblotting analyses for organelle-specific markers: ER (calnexin), mitochondria (complex IV), Golgi apparatus (FTCD), and nuclei (Oct-1).

Immunoblotting Analyses—INS-1 cells were harvested at various times (0–24 h) following induction of ER stress, sonicated, and the homogenate centrifuged (100,000 $\times$ *g*, 1 h, 4 °C) to obtain cytosol. To examine mitochondrial apoptotic factors, the mitochondrial fraction was prepared as described above. An aliquot (30 μg) of cytosolic or mitochondrial protein was analyzed by SDS-PAGE (8 or 15%), transferred onto Immobilin-P polyvinylidene difluoride membranes, and processed for immunoblotting analyses, as described (35). The targeted factors and the primary antibody concentrations were as follows: PERK (1:1000), pPERK (1:1000), eIF2a (1:500), peIF2a (1:1000),

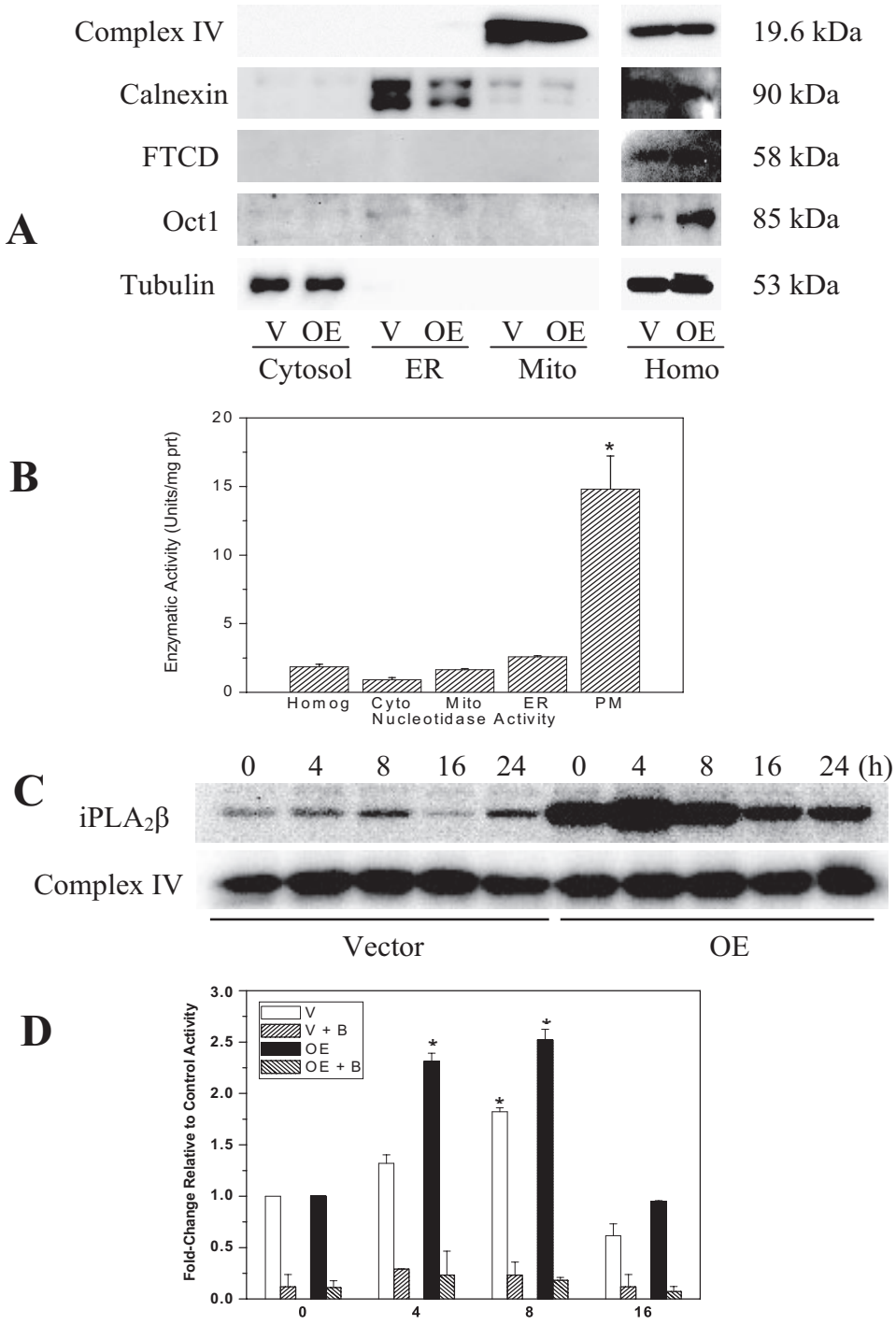

FIGURE 2. **Mitochondrial association of iPLA$_2$β protein and activity during ER stress.** INS-1 cells were treated with either vehicle (*DMSO*) or with thapsigargin (1 μM) and incubated for up to 16–24 h. Cells were harvested at various times and mitochondrial fractions prepared for iPLA$_2$β immunoblotting and phospholipase activity analyses. *A*, verification of mitochondrial fraction purity. Fractions designated cytosol, ER, mitochondria (*Mito*), and homogenate (*Homog*) were probed with organelle-specific markers complex IV (mitochondria), calnexin (ER), FTCD (Golgi), or Oct-1 (nuclei). Tubulin immunoreactivity was used as control. *B*, 5′-nucleotidase activity. Plasma membrane-associated nucleotidase activity was determined in Vector and OE INS-1 cell subcellular fractions using a spectrophotometric method. Because the values were similar in the two groups, they were pooled to determine mean activity (units/mg of protein) in each fraction ($n = 4–6$), where 1 unit is defined as the amount that will hydrolyze 1.0 μmol of inorganic phosphorus from adenosine 5′-monophosphate per min at pH 9.0 at 37 °C. *C*, mitochondria-associated iPLA$_2$β protein. Accumulation of iPLA$_2$β protein in the mitochondria was examined following induction of ER stress (*top panel*) by immunoblotting analyses. Complex IV was used as control (*bottom panel*). *D*, mitochondria-associated iPLA$_2$β activity. Specific iPLA$_2$β catalytic activity in mitochondria prepared from vehicle and thapsigargin-treated INS-1 cells was determined in the absence or presence of BEL (*B*, 1 μM) and expressed as the mean ± S.E. of percent change in activity, relative to corresponding vehicle control activity. Each analysis was done three times (*V* or Vector, empty vector-transfected and OE, iPLA$_2$β-overexpressing INS-1 cells). *, significantly different from corresponding control activity, $p < 0.05$.

iPLA$_2$β (T-14; 1:500), calnexin (1:1,000), FTCD (1:1500), complex IV (1:2,000), Oct-1 (1:1,000), cytochrome *c* (1:1,000), caspase-12 and caspase-3 (1:1,000), and tubulin (1:2000). The secondary antibody concentration was 1:10,000. Immunoreactive bands were visualized by enhanced chemiluminescence (ECL).

Measurement of 5′-Nucleotidase Activity—A spectrophotometric enzymatic assay was used to measure the activity of the plasma membrane enzyme 5′-nucleotidase, according to instructions provided by Sigma (EC 3.1.3.5). This procedure measures the 5′-nucleotidase-mediated liberation of inorganic phosphorous from 5′-AMP, as reflected by monitoring absorbance at 660 nm.

Assay for iPLA$_2$β Activity in the Mitochondria—Mitochondrial fraction was prepared from INS-1 cells harvested at 4, 8, and 16 h following induction of ER stress. Protein concentration was determined using Coomassie reagent. Ca^{2+}-independent PLA_2 activity in an aliquot of mitochondrial protein (30 μg) was assayed under zero Ca^{2+} conditions (no added Ca^{2+} plus 10 mM EGTA) in the presence of [^{14}C]PLPC (5 μM) as the substrate, and specific enzymatic activity was quantitated, as described (35). To verify that the mitochondrial phospholipase activity is manifested by iPLA$_2$β, activity was also assayed in the presence of BEL (1 μM).

Ceramide Analyses by ESI/MS/MS—Lipids were extracted from the mitochondria and ER of INS-1 cells under acidic conditions, as described (34, 35). Briefly, extraction buffer (chloroform, methanol, 2% acetic acid, 2/2/1.8; v/v/v) containing C8-ceramide (*m*/*z* 432) internal standard (500 ng), which is not an endogenous component of INS-1 cell lipids, was added to each fraction of mitochondria and ER. After vigorous vortexing, the mixture was centrifuged (800 × *g*, 5 min, room temperature) and the organic bottom layer collected, concentrated to dryness under nitrogen, and reconstituted in chloroform/methanol (1:4) con-

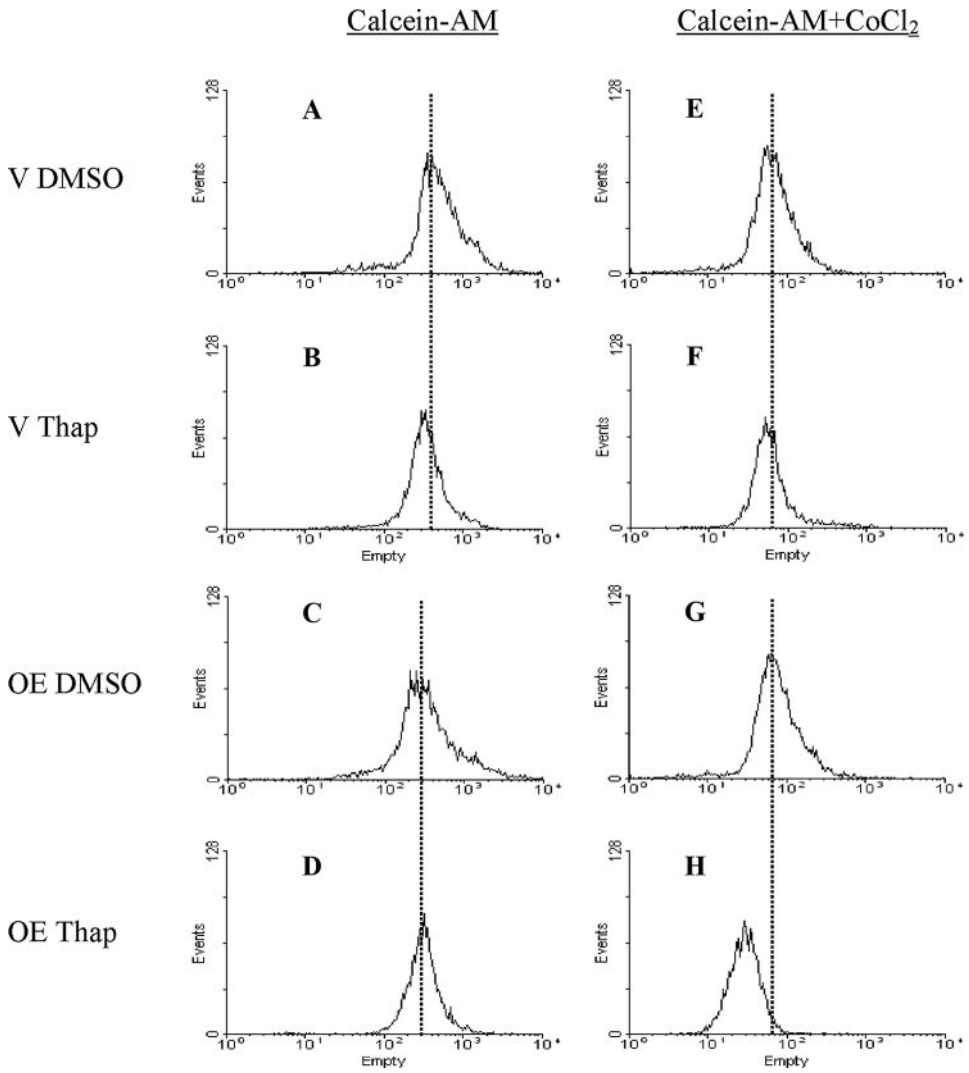

FIGURE 3. **Activation (opening) of mitochondrial PTP during ER stress.** INS-1 cells were treated with either vehicle (*DMSO*) or with thapsigargin (*Thap*) (1 μM) and incubated for 16 h. The cells were then incubated with calcein-AM alone (*panels A–D*) or with calcein-AM and quenching agent $CoCl_2$ (*panels E–H*) and analyzed by flow cytometry. The left-ward shift in fluorescence intensity between *panels E* (DMSO) and *F* (thapsigargin) and *panels G* (*DMSO*) and *H* (*Thap*) reflect PTP opening in Vector (*V*) and OE INS-1 cells, respectively, during ER stress. The *vertical lines* connecting *panels E* and *F* and *panels G* and *H* are presented to show the loss in fluorescence due to PTP activation in ER-stressed cells, relative to control cells. Representative fluorescence spectra generated from analyses of 10,000 INS-1 cells from each experiment are presented. Each analysis was done three to five times (*V*, empty vector-transfected and OE, iPLA$_2\beta$-overexpressing INS-1 cells).

taining 10 pmol/μl of LiOH. The relative abundance of individual ceramide species, relative to the C8-ceramide internal standard, in the mitochondria and ER were determined separately by ESI/MS/MS scanning for constant neutral loss of 48, which reflects the elimination of formaldehyde and water from the $[M + Li^+]$ ion (49). This loss is characteristic of ceramide-Li^+ adducts upon low energy collisionally activated dissociation ESI/MS/MS (50). To measure ceramide content, ESI/MS/MS standard curves were generated from a series of samples containing a fixed amount of C8-CM standard and varied amounts of long chain CM standards, as described (35). Total (pmol) ceramide species in each fraction was determined and normalized to milligrams of protein. Changes between control and treated ER and mitochondrial fractions on each experimental day were combined and mean differences ± S.E. over 7 separate experimental analyses in each group were determined.

Sphingomyelin (SM) Analyses by ESI/MS/MS—Sphingomyelins are formed by reaction of a ceramide with CDP-choline and similar to GPC lipids, they contain a phosphocholine as the polar head group. This feature of sphingomyelins facilitates identification of sphingomyelin molecular species by constant neutral loss scanning of trimethylamine ($[M + H]^+ - N(CH_3)_3$) or constant neutral loss of 59, as described (34). The prominent ions in the total ion current spectrum are those of the even mass PC molecular species and these mask the odd mass sphingomyelin signals (34). Constant neutral loss of 59, however, facilitates emergence of signals for sphingomyelin species at odd m/z values, reflecting loss of nitrogen. Lipid extracts were prepared as above in the presence of 14:0/14:0-GPC (m/z 684, 8 μg) as internal standard, which is not an endogenous component of INS-1 cell lipids, and analyzed by ESI/MS/MS. Sphingomyelin content in the samples was determined based on standard curves generated using commercially available brain and egg sphingomyelins with a known percentage of each fatty acid constituent and 14:0/14:0-GPC (m/z 684, 8 μg) as internal standard, as described (34). Total (pmol) sphingomyelin species in each fraction was determined and normalized to milligrams of protein. Changes between control and treated ER and mitochondrial fractions on each experimental day were combined and mean differences ± S.E. over 7 separate experimental analyses in each group were determined.

Statistical Analyses—Data were converted to mean ± S.E. values and the Student's t test was applied to determine significant differences between two samples ($p < 0.05$). Statistical differences between multiple treatment groups and a control group were determined using analysis of variance and Dunnett post-hoc test. The n value for each analysis is indicted in the figure legends.

RESULTS

Induction of ER stress with thapsigargin causes an increase in ceramide generation and INS-1 cell apoptosis that are both suppressed by inactivation of iPLA$_2\beta$ with BEL (34, 35). Such

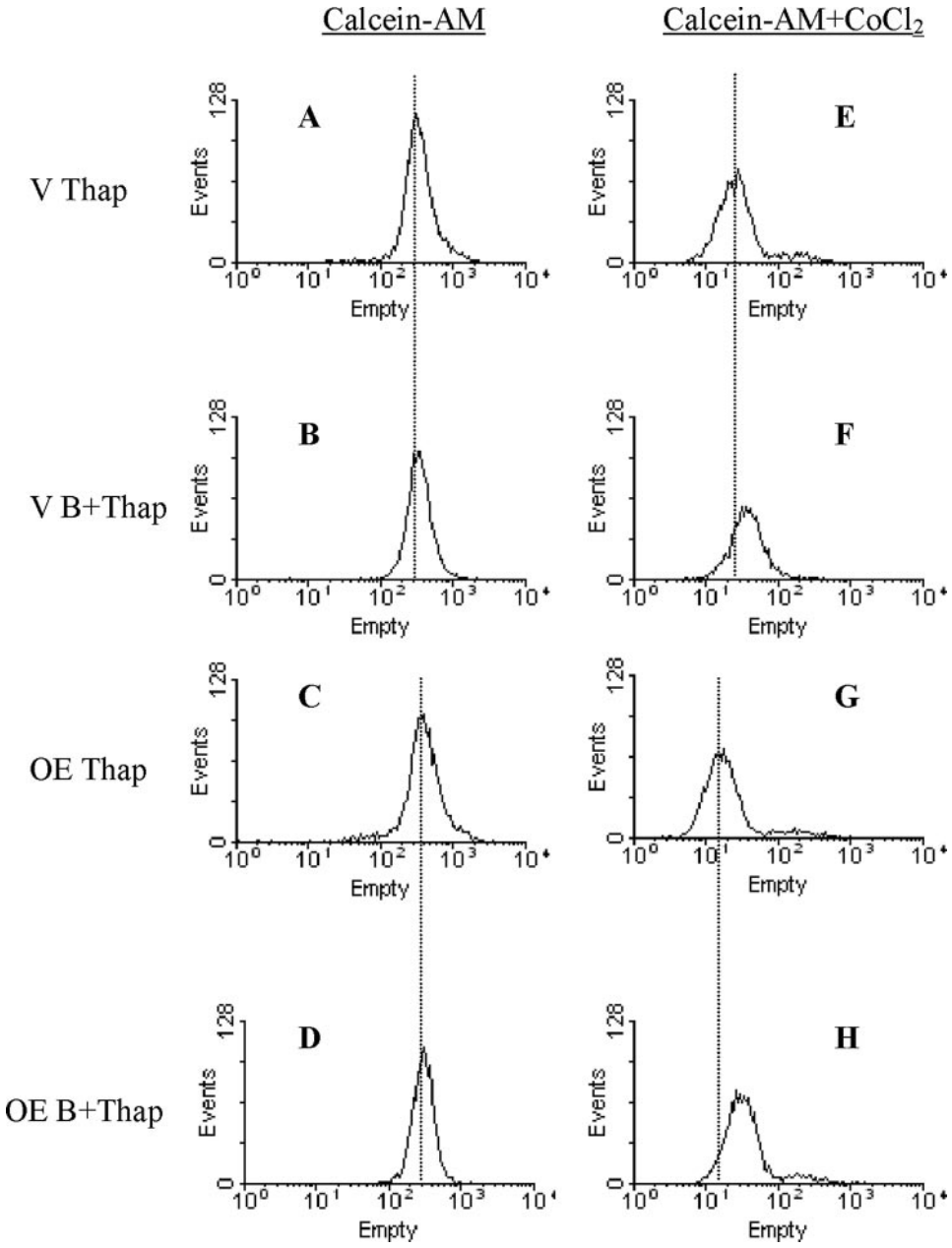

FIGURE 4. **Inhibition of ER stress-induced changes in PTP by BEL.** INS-1 cells were pretreated with either DMSO vehicle or BEL (*B*, 1 μM) for 1 h. The medium was then replaced with one containing thapsigargin (*Thap*, 1 μM). At 16 h, the cells were harvested and processed for PTP analyses, as described in the legend to Fig. 3. *Panels A–D*, calcein-AM alone. *Panels E–H*, calcein-AM + $CoCl_2$. The right-ward shifts in calcein-AM fluorescence spectra between *panels E* (*Thap*) and *F* (*B*+*Thap*) and *panels G* (*Thap*) and *H* (*B*+*Thap*) indicate reversal of ER stress-induced PTP opening in Vector (*V*) and OE INS-1 cells, respectively. The *vertical lines* connecting *panels E* and *F* and *panels G* and *H* are presented to show the reversal in fluorescence loss due to inhibition of PTP activation in ER-stressed cells pretreated with BEL, relative to Thap alone-treated cells. Representative fluorescence spectra generated from analyses of 10,000 INS-1 cells from each experiment by flow cytometry are presented. Each analysis was done three to five times (*V*, empty vector-transfected and OE, iPLA$_2\beta$-overexpressing INS-1 cells).

findings indicate that iPLA$_2\beta$ participates in ER stress-induced apoptosis but the precise mechanism by which iPLA$_2\beta$ and ceramides contribute to apoptosis of insulin-secreting cells remains unclear. We examined this issue in the present study by comparing the effects of ER stress in empty vector (Vector) and iPLA$_2\beta$ cDNA vector (OE) construct-transfected INS-1 cells. The OE cells express a 10-fold higher iPLA$_2\beta$ catalytic activity, are more sensitive to ER stress, and exhibit amplified apoptosis, relative to Vector cells, which are inhibitable by BEL (34, 35).

ER Stress Induces ER and Mitochondrial Factors—Because ER stress promoted a loss in $\Delta\Psi$ in addition to inducing ER stress factors CHOP and BiP (34, 35), we examined the appearance of mitochondrial apoptotic factors during ER stress-induced INS-1 cell apoptosis. Vector and OE cells were treated with thapsigargin and harvested at various times for immunoblotting analyses of ER and mitochondrial-related factors. As expected, ER stress led to phosphorylation of pancreatic ER kinase-like ER kinase (PERK) and of its downstream substrate eukaryotic initiation factor 2 (eIF2a), and activation of caspase-12 (Fig. 1*A*). Activation of PERK and eIF2a occurs earlier and is amplified in OE INS-1 cells, relative to Vector only cells, but cleavage of caspase-12 to its active 42-kDa form does not appear to be similarly amplified by iPLA$_2\beta$ overexpression. ER stress also promoted the release of cytochrome *c* and Smac from the mitochondria (Fig. 1*B*) and their accumulation in the cytosol, hallmark signs of mitochondrial decompensation, is amplified in the OE cells, relative to Vector cells. Consistent with the induction of apoptosis due to ER stress and its amplification in INS-1 cells overexpressing iPLA$_2\beta$, activation of the executioner caspase-3, as reflected by its cleavage to the 19-kDa form, is evident between 16 and 24 h (Fig. 1*C*) with greater activation occurring in the OE cells, relative to Vector cells. Representative quantitation of the bands is presented on the right (*D panels*). These findings raise the possibility that a role for iPLA$_2\beta$ in the ER stress-mediated apoptotic process may involve activation of the mitochondria.

Accumulation of Mitochondria-associated iPLA$_2\beta$ Protein and Activity during ER Stress—To determine if ER stress-induced mitochondrial perturbations are associated with increased mitochondrial association of iPLA$_2\beta$, a mitochondrial fraction was prepared using a douncing protocol. Purity of the fraction was assessed first and as illustrated in Fig. 2, *A* and

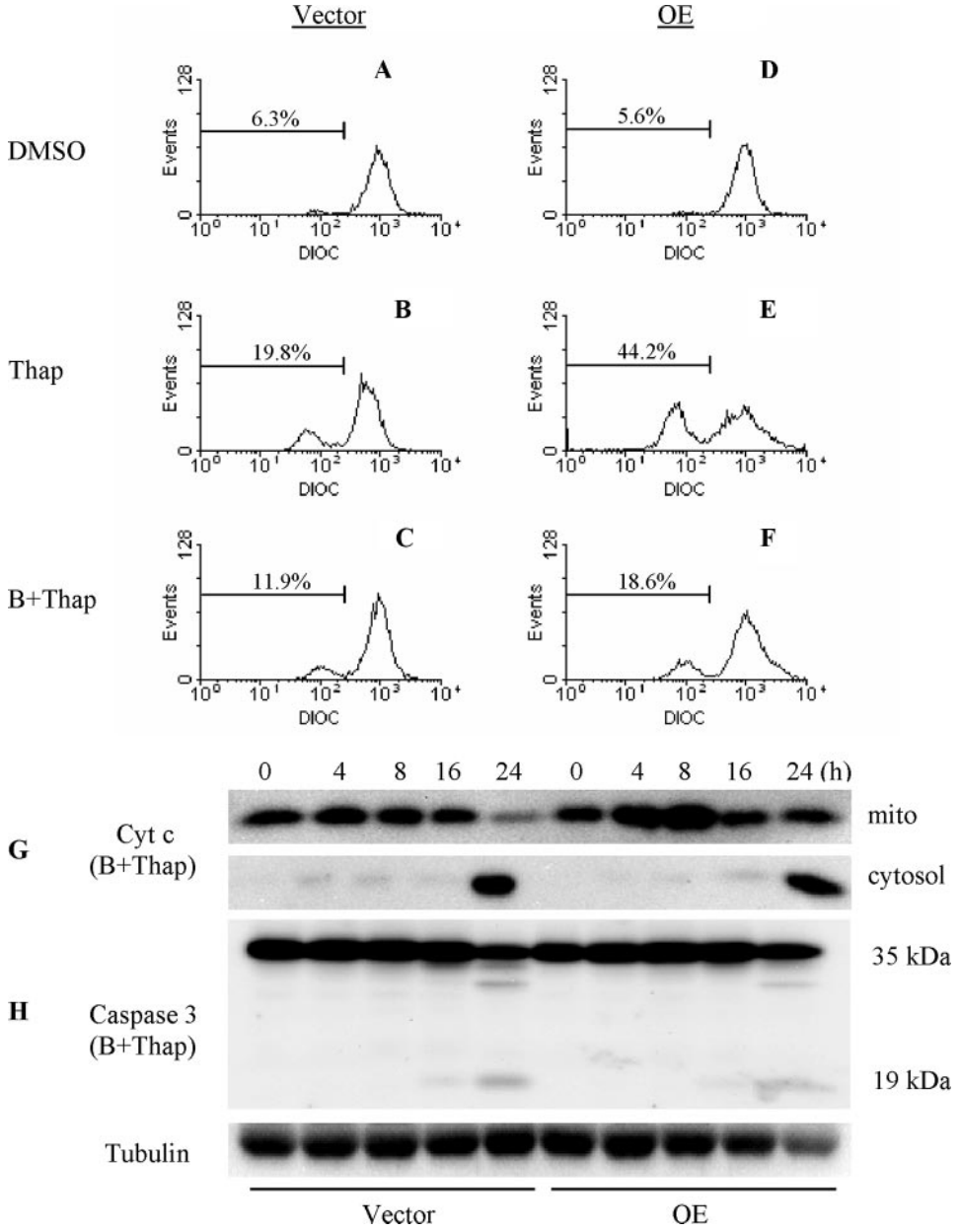

FIGURE 5. **Inhibition of ER stress-induced decrease in mitochondrial membrane potential ($\Delta\Psi$), cytochrome (*cyt*) *c* release, and caspase-3 activation by BEL.** *A–F*, INS-1 cells were pretreated with either vehicle (*DMSO*) or BEL (*B*, 1 μM) for 1 h. The medium was then replaced with one containing with thapsigargin (*Thap*, 1 μM). At 16 h, the cells were harvested and processed for $\Delta\Psi$ analyses. Representative fluorescence spectra generated from analyses of 10,000 INS-1 cells from each experiment by flow cytometry are presented. The percentage of cells (mean of four separate experiments) in which $\Delta\Psi$ is compromised is indicated in each panel. *G*, immunoblot analyses of cytochrome *c* in cytosol and mitochondria. *H*, immunoblot analyses of caspase-3 in homogenates. Tubulin immunoreactivity was used as control. Each analysis was done three to four times (*V*, empty vector-transfected and OE, iPLA$_2\beta$-overexpressing INS-1 cells).

B, the homogenate, as expected, contained all organelle markers. However, the fraction designated mitochondria is enriched in complex IV but not in calnexin, FTCD, Oct-1, or 5′-nucleotidase activity. These findings verified that this fraction is predominantly comprised of mitochondria and does not contain significant amounts of ER, Golgi, nuclei, or plasma membrane, respectively. ER stress was then induced in INS-1 cells and at various times the cells were harvested and mitochondrial fractions prepared for iPLA$_2\beta$ protein and activity assays. Following induction of ER stress, iPLA$_2\beta$ accumulation in the mitochondria increases gradually and peak levels of iPLA$_2\beta$ protein (Fig. 2*C*) and activity (Fig. 2*D*) are reached in the Vector cells at 8 h and in the OE cells at 4 h. The measured catalytic activity is found to be sensitive to inhibition with BEL, providing evidence for ER stress-promoted accumulation of iPLA$_2\beta$ in the mitochondria.

Activation of PTP during ER Stress—Because PTP opening can lead to loss in $\Delta\Psi$ and cytochrome *c* release (46) and we find that ER stress promotes loss in $\Delta\Psi$ (34), cytochrome *c* release, and accumulation of iPLA$_2\beta$ in the mitochondria we examined whether ER stress leads to PTP activation in INS-1 cells and if it is influenced by iPLA$_2\beta$ expression. PTP activation was examined in intact INS-1 cells by a flow cytometry assay based on monitoring fluorescence of calcein-AM entrapped in the mitochondria through Co^{2+} quenching of cytosolic calcein fluorescence (51). ER stress was induced in Vector and OE INS-1 cells and at 16 h the cells were harvested and loaded with calcein-AM in the absence or presence of $CoCl_2$ and its fluorescence was detected after a 15-min incubation period. The 16-h time point is presented because it corresponded to the time when near maximal cytochrome *c* release is observed (Fig. 1*B*). Each spectrum presented in Fig. 3 reflects fluorescence measurement in 10,000 cells. In the absence of the quenching agent, calcein-AM accumulates in the cytosol (*panels A–D*). Addition of $CoCl_2$, due to the quenching effects of Co^{2+}, reduces the overall fluorescence and this is reflected by the left-ward shift in the spectra (*panels E–H*), relative to the corresponding unquenched left set of panels. In cells in which ER stress is induced and are undergoing apoptosis (*panels F* and *H*), the fluorescence signal is further reduced, relative to corresponding control cells (*panels E* and *G*). Comparison of *panels F* and *H* illustrates that activation of PTP is greater in the OE cells, relative to Vector cells. These findings suggest that ER stress leads to PTP activation and that this process can be modulated by iPLA$_2\beta$.

Inhibition of ER Stress-induced PTP Opening by iPLA$_2\beta$ Inactivation—To verify a role for iPLA$_2\beta$ in the PTP activation pathway during ER stress, Vector and OE cells were incubated

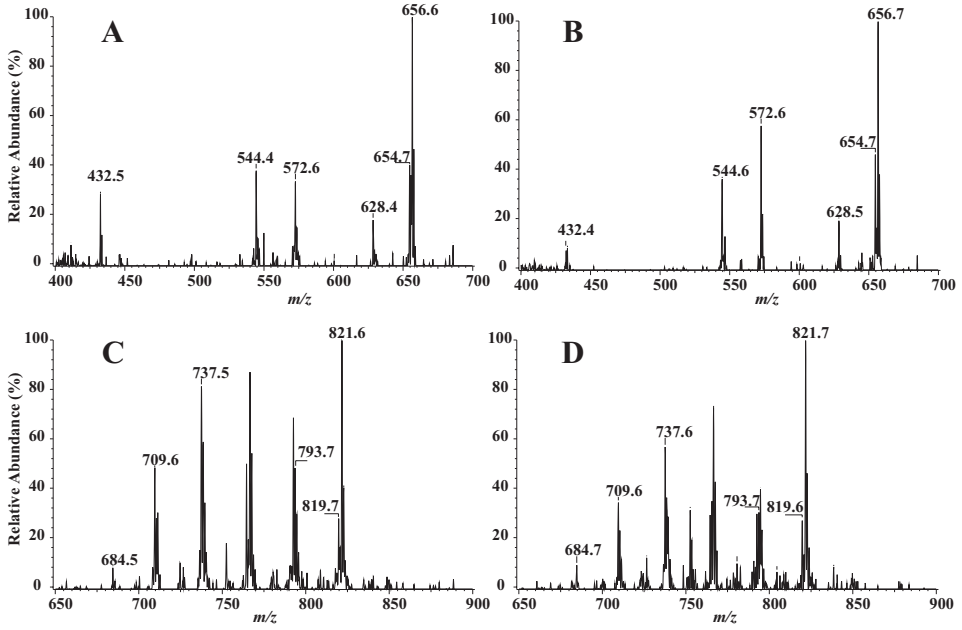

FIGURE 6. **Ceramide and sphingomyelin analyses in the mitochondrial fraction by ESI mass spectrometry.** OE INS-1 cells were treated with vehicle (*DMSO*, control) or with thapsigargin (1 μM) for 20 h. The cells were then detached and mitochondria fraction was prepared. Lipids from each were extracted in the presence of C8-ceramide internal standard (*m/z* 432) or (14:0/14:0)-GPC internal standard (*m/z* 684). The relative abundance of ceramide (*panels A* and *B*) and sphingomyelin (*panels C* and *D*) molecular species were then separately analyzed by ESI/MS/MS by monitoring constant neutral loss scanning of 48 and 59, respectively. *A* and *C*, OE control. *B* and *D*, OE + thapsigargin (*Thap*). The major ceramide molecular species (16:0 (*m/z* 544), 18:0 (*m/z* 572), 22:0 (*m/z* 628), 24:1 (*m/z* 654), and 24:0 (*m/z* 656)) and sphingomyelin molecular species (16:0 (*m/z* 709), 18:0 (*m/z* 737), 22:0 (*m/z* 793), 24:1 (*m/z* 819) and 24:0 (*m/z* 821)) are indicated in each spectrum. Each analysis was done seven times.

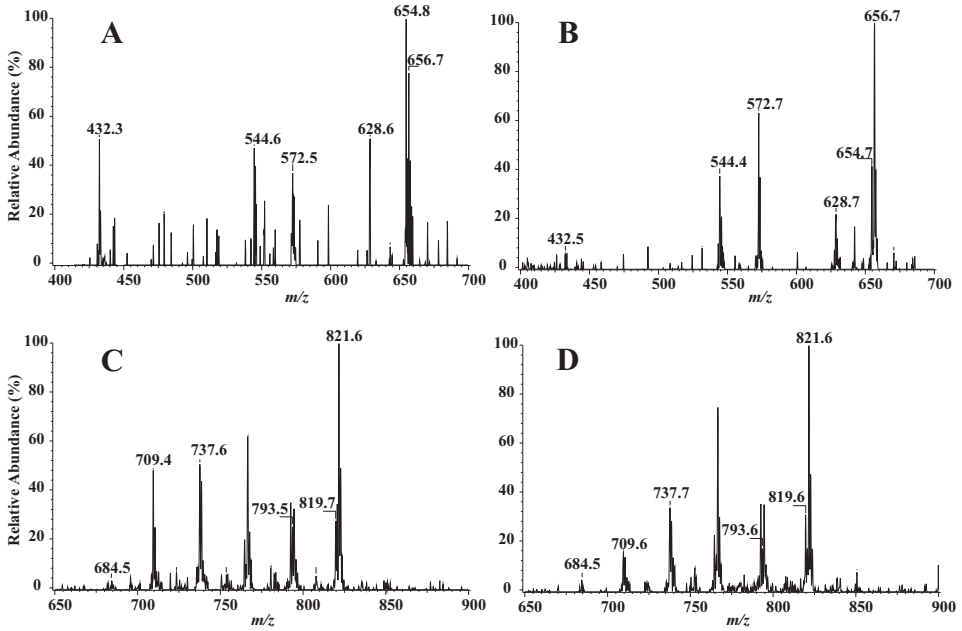

FIGURE 7. **Ceramide and sphingomyelin analyses in the ER fraction by ESI mass spectrometry.** OE INS-1 cells were treated with vehicle (DMSO, control) or thapsigargin (*Thap*) (1 μM) for 20 h. The cells were then detached and the ER fraction was prepared. Lipids from each were extracted in the presence of C8-ceramide internal standard (*m/z* 432) or (14:0/14:0)-GPC internal standard (*m/z* 684). The relative abundance of ceramide (*panels A* and *B*) and sphingomyelin (*panels C* and *D*) molecular species were then analyzed and indicated in each spectrum as described in the legend to Fig. 6. *A* and *C*, OE control. *B* and *D*, OE + thapsigargin. Each analysis was done seven times.

without or with BEL for 1 h prior to induction of ER stress. PTP opening was then examined at 16 h and the results are presented in Fig. 4. At concentrations that completely abolish iPLA$_2\beta$ activity and suppress ER stress-induced INS-1 cell apoptosis (35), BEL alone did not affect PTP (data not shown). However, pretreatment with BEL reversed the reduction in calcein-AM fluorescence promoted by ER stress. This is reflected by the right-ward shifts in peak fluorescence in the Vector (*panels E versus F*) and OE (*panels G versus H*) cells. These findings are consistent with iPLA$_2\beta$ activation contributing to PTP opening during ER stress.

Inhibition of ER Stress-induced Decrease in $\Delta\Psi$, Cytochrome c Release, and Caspase-3 Activation by iPLA$_2\beta$ Inactivation—Opening of PTP can lead to downstream events that include loss in $\Delta\Psi$, release of cytochrome *c*, and activation of caspases. To examine if these events are sensitive to iPLA$_2\beta$ activation, Vector and OE cells were incubated without or with BEL for 1 h prior to induction of ER stress. At 16 h, $\Delta\Psi$ was measured in a suspension of cells to which a fluorescent Mito Flow reagent was added. This reagent concentrates in the mitochondria of healthy cells but the mitochondria of cells undergoing apoptosis become compromised and accumulate less of the reagent and this is reflected by a decrease in the fluorescence signal and the appearance of a second peak that is left of the original. The spectra presented in Fig. 5, *A–F*, reflect fluorescence measurement in 10,000 INS-1 cells and the percentage of cells (mean of 4 separate experiments) losing $\Delta\Psi$ was analyzed by the application software and is indicated as M1. As illustrated, only a small percentage (5–6%) of cells are decompensated with vehicle alone (*panels A* and *D*) but induction of ER stress causes a loss in $\Delta\Psi$ that is 3-fold greater in Vector cells (*panel B*) and 9-fold greater in OE cells (*panel E*), relative to vehicle-treated cells. BEL alone does not affect $\Delta\Psi$ (data not shown) but its addition suppresses the percentage of cells with compromised $\Delta\Psi$ (*panel C versus F*). Consistent with its inhibitory effects on ER stress-induced changes in PTP and $\Delta\Psi$, BEL treatment prevents cytochrome *c* release through 16 h

(*panel G*) and suppresses activation of the apoptosis executioner caspase-3 (*panel H*). The findings presented in Figs. 1–5 therefore indicate that the mitochondria-associated apoptotic pathway is invoked during ER stress and that iPLA$_2\beta$ activation provides signals essential to this process.

ER Stress Induces Ceramide Generation in the Mitochondrial and ER Fractions—Ceramides are recognized to affect PTP (52, 53) and their increased generation has been observed in ER-stressed INS-1 cells (34, 35). Total cellular ceramide accumulation during ER stress was previously determined, using inhibitors of serine palmitoyltransferase and neutral sphingomyelinase (NSMase), to occur via iPLA$_2\beta$-mediated hydrolysis of sphingomyelins by NSMase (34, 35). Here, we examined whether ER stress promotes ceramide generation in the ER and mitochondria of INS-1 cells via sphingomyelin hydrolysis. The ER fraction was prepared, as described above, and assessed for purity. As shown in Fig. 2, *A* and *B*, this fraction was found to be enriched in calnexin but not other organelle markers. The choice of the 20-h time point was based on the combination of findings reported earlier (34, 35) indicating that NSMase expression, ceramide generation, and apoptosis are near maximal between 16 and 24 h following induction of ER stress.

Ceramide (CM) species were measured as their Li^+ adducts (34, 35) relative to the internal standard C8-CM, which contains an octanoic acid residue as the fatty amide substituent. Figs. 6 and 7 (*panels A* and *B*) display representative positive ion ESI-MS total ion current tracings of Li^+ adducts of the CM species in mitochondrial and ER fractions, respectively, after addition of the C8-CM internal standard, which is represented in the spectrum by its $[M + Li^+]^+$ ion (*m*/*z* 432). The fatty amide substituents of the major CM species endogenous to INS-1 cells are 16:0 (*m*/*z* 544), 18:0 (*m*/*z* 572), 22:0 (*m*/*z* 628), 24:1 (*m*/*z* 654), and 24:0 (*m*/*z* 656). The spectra were acquired by monitoring constant neutral loss of 48 in OE INS-1 cells treated with either vehicle (*panels A*) or thapsigargin (*panels B*). As illustrated, following induction of ER stress, the relative abundances of the CM molecular species in INS-1 cells are higher in both the mitochondria and ER fractions, as reflected by the increases in intensity of ions representing them.

Figs. 6 and 7 (*panels C* and *D*) display representative positive ion ESI-MS total ion current tracings of Li^+ adducts of the sphingomyelin species in mitochondrial and ER fractions, respectively, after addition of the 14:0/14:0-GPC internal standard, which is represented in the spectrum by its $[M + Li^+]^+$ ion (*m*/*z* 684). As with the ceramide species, the major sphingomyelin species endogenous to INS-1 cells are 16:0 (*m*/*z* 709), 18:0 (*m*/*z* 737), 22:0 (*m*/*z* 693), 24:1 (*m*/*z* 819), and 24:0 (*m*/*z* 821). The spectra were acquired by monitoring constant neutral loss of 59, as described (54), in OE INS-1 cells treated with either vehicle (*panels C*) or thapsigargin (*panels D*). As illustrated, following induction of ER stress, the relative abundance of the sphingomyelin molecular species in INS-1 cells are lower in both the mitochondria and ER fractions, as reflected by the decreases in the intensity of ions representing them.

Differences in the combined (ER + mitochondria) pool of ceramides and sphingomyelins (picomole/mg of protein) between vehicle- and thapsigargin-treated groups are shown in Fig. 8. As seen, ceramides increased and sphingomyelins

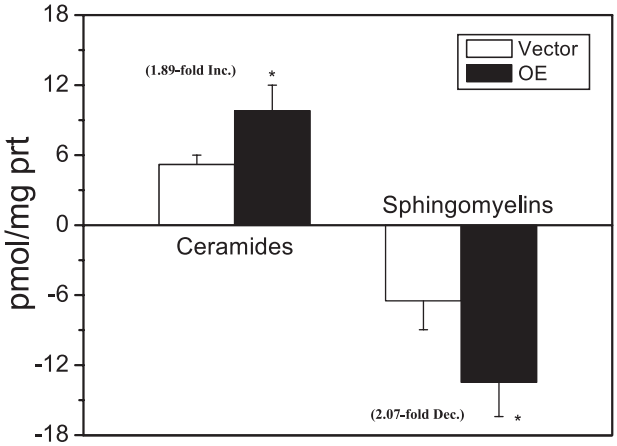

FIGURE 8. **ER stress-induced ceramide generation and sphingomyelin hydrolysis in the mitochondrial and ER fractions.** Vector and OE INS-1 cells were treated with either vehicle (DMSO, Control) or thapsigargin (1 μM) for 20 h. The cells were then harvested, ER and mitochondria fractions prepared, and lipids in each fraction extracted separately in the presence of internal standards C8-ceramide (*m*/*z* 432) or 14:0/14:0-GPC (*m*/*z* 684). An aliquot of each fraction was then used separately to determine the relative abundance of ceramide and sphingomyelin molecular species by ESI/MS/MS. Total (pmol) ceramide and sphingomyelin molecular species in each fraction were then determined and normalized to milligrams of protein, as described under "Experimental Procedures." (Vector (*V*) and OE pools of ceramides (nmol/mg protein): VC, 3.52 ± 1.20 and VT, 8.63 ± 1.46; OEC, 2.47 ± 0.54 and OET, 11.69 ± 2.59; V and OE pools of sphingomyelins (nmol/mg of protein): VC, 35.53 ± 6.35 and VT, 28.96 ± 9.52; OEC, 38.24 ± 10.80 and OET, 25.32 ± 5.69).) The change in the pool of ceramides and sphingomyelins between control and treated ER and mitochondria fractions on each experimental day were used to calculate the presented mean differences ± S.E. ($n = 7$ in each group). The *numbers in parentheses* indicate the –fold change in the OE pools, relative to the Vector pools (Vector, empty vector-transfected and OE, iPLA$_2\beta$-overexpressing INS-1 cells). *, OE pool significantly different from corresponding Vector pool, $p < 0.05$.

decreased following induction of ER stress in both Vector and OE groups. However, such changes were nearly 2-fold greater in the OE group, relative to the Vector group. Comparison of the incremental changes revealed that the magnitude of change in ceramides is similar to the magnitude of change in sphingomyelins in both groups (CMs *versus* SMs: Vector, $p = 0.6269$ and OE, $p = 0.4157$). These findings therefore are consistent with ceramide generation via sphingomyelin hydrolysis following induction of ER stress.

Ceramide- and ER Stress-induced Cell Death Is Suppressed by Forskolin—In view of ceramide accumulation during ER stress, direct effects of C2-ceramide were compared with ER stress-induced effects. As shown in Fig. 9*A*, addition of C2-ceramide induces INS-1 cell apoptosis, as reflected by the greater abundance of TUNEL-positive cells treated with the ceramide, relative to vehicle-treated cells. Elevations in cAMP content have a suppressing effect on ceramide-induced cell death (55) and in agreement with those studies, addition of the adenylate cyclase activator forskolin results in significant reductions (~50%) in ceramide-induced INS-1 cell apoptosis (Fig. 9, *A* and *C*). If iPLA$_2\beta$-mediated ceramide generation during ER stress contributes to cell death, it might be speculated that addition of forskolin should reduce ER stress-induced apoptosis. As shown in Fig. 9, *B* and *D*, this is indeed what is observed as ER stress-induced INS-1 cell apoptosis is also inhibited nearly 50% by forskolin. These findings suggest that ceramides generated dur-

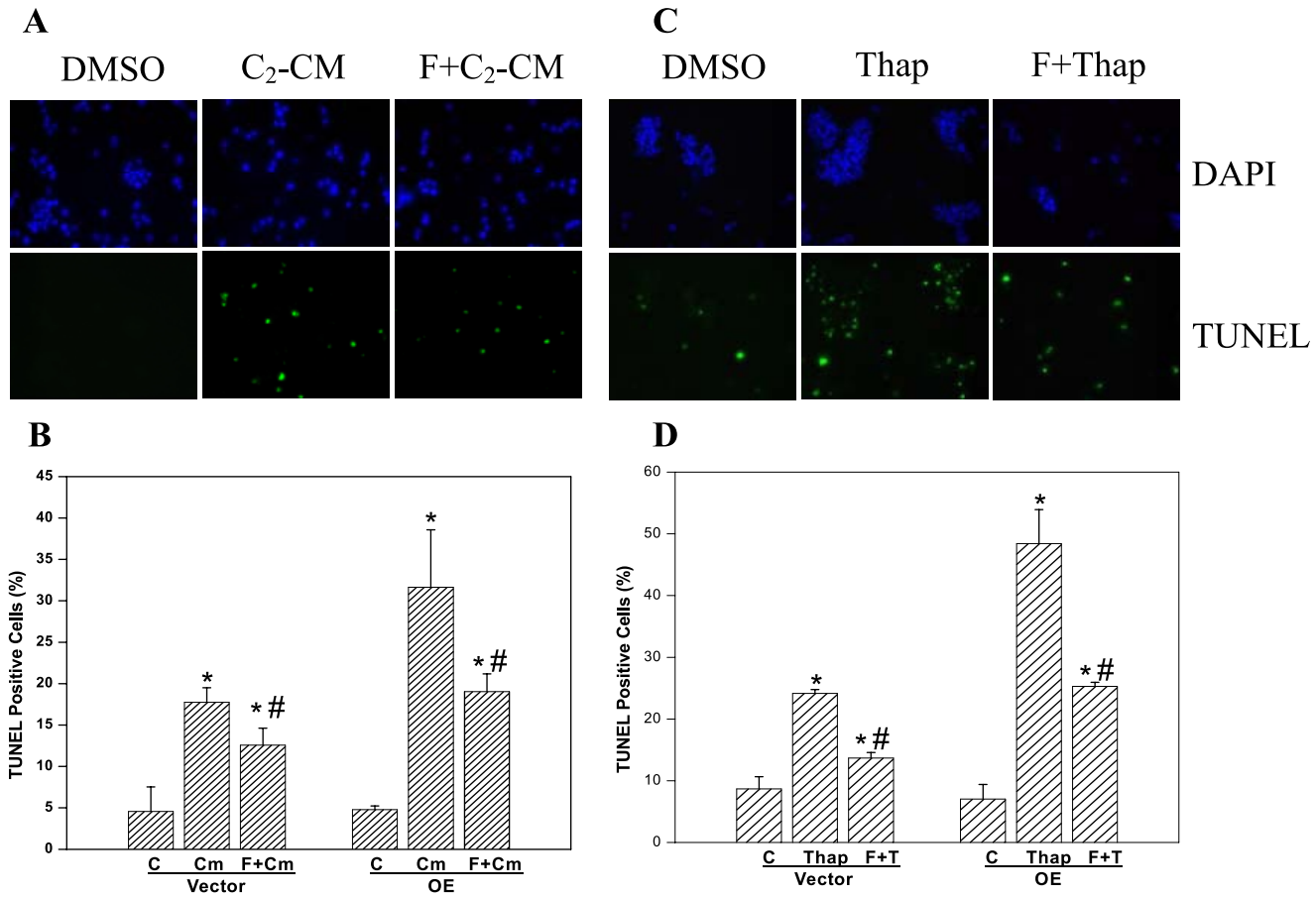

FIGURE 9. **Ceramide- and ER stress-induced INS-1 cell apoptosis is suppressed by forskolin.** INS-1 cells were treated with vehicle (DMSO, control), C2-ceramide (C2-CM, 50 μM), or with thapsigargin (*Thap*, 1 μM) following preincubation in the absence or presence of forskolin (*F*, 2.5 μM, 1 h). *A* and *C*, DAPI and TUNEL staining. The cells were harvested at 16 h, processed for staining of cellular nuclei and cells undergoing apoptosis, and visualized by fluorescence microscopy. *B* and *D*, quantitation of TUNEL-positive apoptotic cells. Total cell number (DAPI-stained) and apoptotic cell number (TUNEL-positive cells) in a field of a slide were counted. A minimum of 5 fields per slide ($n = 3$) were analyzed and mean percentages ± S.E. of apoptotic cells, relative to total cell number, are presented. *, significantly different from corresponding control. #, significantly different from corresponding C2-CM or thapsigargin group, $p < 0.05$, $n = 3$–7 slides in each group). Vector, empty vector-transfected and OE, iPLA$_2\beta$-overexpressing INS-1 cells.

ing ER stress can play a key role in the pathway leading to ER stress-induced apoptosis of insulin-secreting cells.

ER Stress-induced Loss in $\Delta\Psi$ *and Cytochrome c Release Are Mediated by Ceramides*—In the absence of differences in caspase-12 activation between Vector and OE INS-1 cells but amplified cytochrome *c* release in the OE cells following induction of ER stress, the possibility that iPLA$_2\beta$ activation leads to mitochondrial decompensation through ceramide generation was examined. INS-1 cells were treated with either C2-ceramide or thapsigargin alone or in combination with forskolin. As shown in Fig. 10, relative to vehicle-treated cells (*panels A* and *G*), the ceramide and ER stress caused loss in $\Delta\Psi$ in Vector (*panels B* and *D*) and OE (*panels H* and *J*) cells and addition of forskolin reduced the percentage of Vector (*panels C* and *E*) and OE (*panels I* and *K*) cells that lose $\Delta\Psi$. The NSMase inhibitor GW4869 also suppressed ER stress-induced loss in $\Delta\Psi$ (*panels F* and *L*) and this was associated with dramatic reductions in cytochrome *c* release in both Vector and OE cells (*panel M*). In light of the earlier observation that inhibition of NSMase prevented ER stress-induced sphingomyelin hydrolysis and ceramide generation in INS-1 cells (34), the present findings suggest that mitochondrial decompensation and consequential release of cytochrome *c* that occur during ER stress are promoted by ceramides generated via iPLA$_2\beta$-mediated activation of NSMase.

DISCUSSION

β-Cell apoptosis can result from prolonged ER stress and such a mechanism is thought to contribute to β-cell death during the development of diabetes mellitus (17). Recent studies indicate that the Group VIA Ca^{2+}-independent phospholipase A_2 (iPLA$_2\beta$) participates in ER stress-induced INS-1 cell apoptosis (34, 35). Of particular interest are the findings in the latter studies that ER stress leads to ceramide generation via the sphingomyelin hydrolysis pathway that is dependent on iPLA$_2\beta$-sensitive induction of NSMase. Although inhibition of NSMase activity or expression or inhibition of iPLA$_2\beta$ prevented ER stress-induced ceramide generation and INS-1 cell apoptosis in those studies, the mechanism(s) by which iPLA$_2\beta$ or ceramides contribute to apoptotic cell death remained unidentified.

As the current understanding of events activated during ER stress-induced cellular events increases, it is being recognized that prolonged ER stress can lead to mitochondrial damage (56,

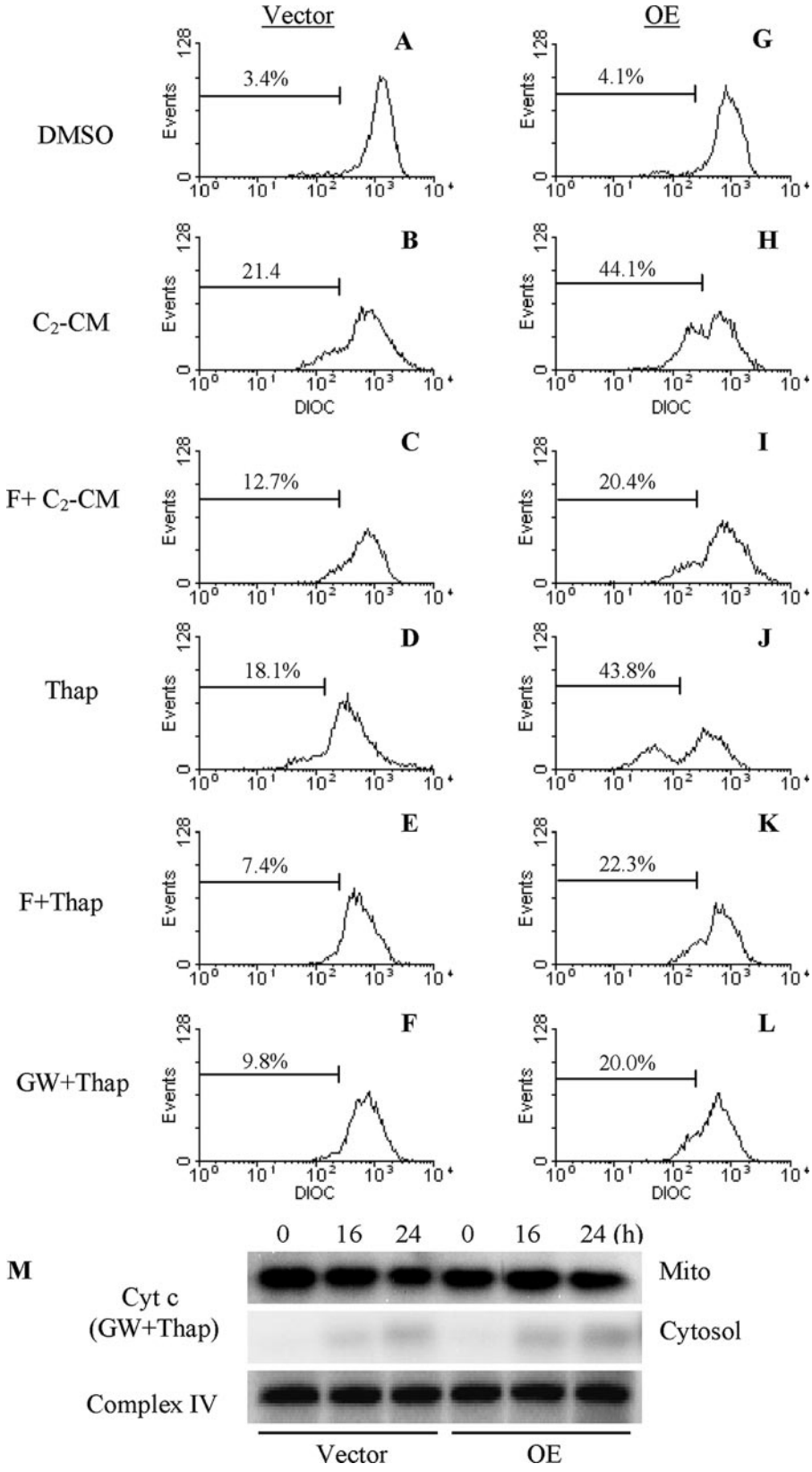

FIGURE 10. **Suppression of ceramide and ER stress-induced ΔΨ loss and cytochrome *c* release.** Vector (*panels A–F*) and OE (*panels G–L*) INS-1 cells were treated with either forskolin (*F*, 2.5 μM) or GW4869 (*GW*, 10 μM) for 1 h prior to addition of thapsigargin (*Thap*, 1 μM) or C2-ceramide (*C2-CM*, 50 μM). At 16 h, the cells were harvested for ΔΨ analyses by flow cytometry. Each analysis was done three to five times. *M*, immunoblot analyses of cytochrome *c* in cytosol and mitochondria prepared from Vector (*V*) and OE INS-1 cells pretreated for 1 h with GW4869 (10 μM) prior to addition of thapsigargin (1 μM). Complex IV immunoreactivity was used as control. Each analysis was done three times. Vector, empty vector-transfected and OE, iPLA$_2\beta$-overexpressing INS-1 cells.

57). A suggested mechanism linking ER stress with the intrinsic apoptotic pathway begins with the release of Ca^{2+} from ER stores into the cytosol during ER stress (57–60). A major Ca^{2+} sequestering organelle is the mitochondria, which uses ruthenium red-sensitive uptake and Na^{+}-Ca^{2+} exchanger pathways to remove Ca^{2+} from the cytosol (31). Accumulation of Ca^{2+} in the mitochondria leads to collapse of ΔΨ, PTP formation, release of cytochrome *c*, and apoptosis-inducing factor (32). The increase in ER Ca^{2+} during stress is proposed to activate calpain leading to cleavage of caspase-12, which is located in the ER (15), into an active form (57). However, recent evidence indicates that ER stress-induced apoptosis can occur via an apoptosome-dependent pathway that does not require caspase-12 activation (61, 62). In agreement with this latter possibility, we find that whereas ER stress-induced INS-1 cell apoptosis is BEL-sensitive, activation of caspase-12 is not affected by iPLA$_2\beta$ expression. This, taken together with the earlier demonstration of amplification of loss in ΔΨ in ER-stressed iPLA$_2\beta$ OE INS-1 cells (34, 35), raises the possibility that apoptosis due to ER stress requires iPLA$_2\beta$-mediated activation of the mitochondria.

Here, we report that iPLA$_2\beta$ activation and subsequent ceramide generation are key components in the cross-talk between the ER and mitochondria following induction of ER stress and that their involvement serves to amplify ER stress-induced apoptosis of insulin-secreting cells. This is based on the findings that (*a*) ER stress leads to iPLA$_2\beta$ association with mitochondria, (*b*) ER stress leads to ceramide generation in both the ER and mitochondrial fractions, (*c*) ceramides induce apoptosis and loss in ΔΨ, analogous to ER stress, and the effects of both ceramides and ER stress are similarly suppressed by forskolin, and (*d*) ER stress leads to PTP opening, loss of ΔΨ, and cytochrome *c* release and these signature mito-

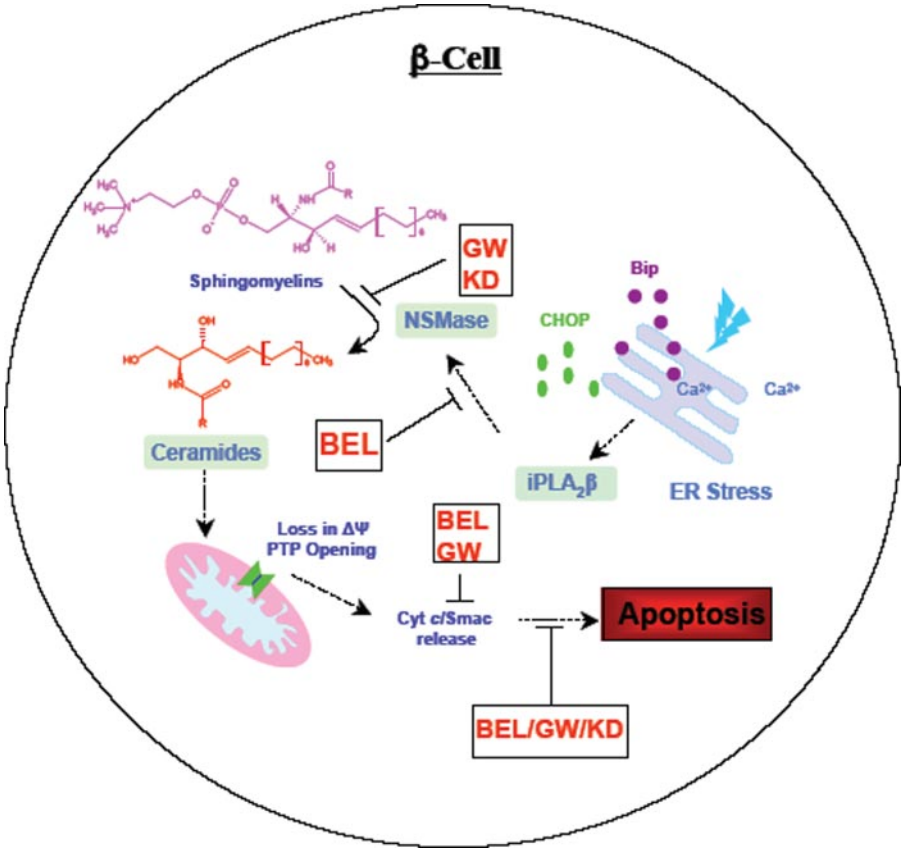

FIGURE 11. **Proposed interplay between iPLA$_2\beta$, ceramides, and mitochondria during ER stress-induced β-cell apoptosis.** During ER stress, the expression/activity of iPLA$_2\beta$ increases, leading to induction of NSMase and increased hydrolysis of sphingomyelins and generation of ceramides. These lipid mediators activate the mitochondrial apoptotic processes and cause loss in $\Delta\Psi$, activation of PTP, and release of cytochrome *c* into the cytosol. The latter interacts with other factors to activate caspases and cause apoptosis of the β-cell. In support of this process, inhibition of iPLA$_2\beta$ BEL suppresses NSMase expression and ceramide generation (34), cytochrome (*Cyt*) *c* release, and apoptosis. Furthermore, chemical inhibition (with GW4869) or knockdown (*KD*) of NSMase suppresses ceramide generation (34), cytochrome *c* release, and apoptosis.

chondria-related events of apoptosis are suppressed by inhibition of iPLA$_2\beta$ or ceramide generation.

Ceramides are recognized to participate in cell survival and apoptosis pathways (42, 43) and inactivation of iPLA$_2\beta$ with BEL inhibits ceramide accumulation and apoptosis due to ER stress (34, 35). We therefore considered the possibility that ceramides generated via an iPLA$_2\beta$-sensitive pathway promote mitochondrial dysfunction during ER stress. We examined this by monitoring PTP, $\Delta\Psi$, and cytochrome *c* release in control and iPLA$_2\beta$ overexpressing INS-1 cells following induction of ER stress. Permeabilization of the outer mitochondrial membrane is considered to be a "point of no return" during apoptosis (63) and PTP opening alters outer mitochondrial membrane permeability. Prolonged activation of PTP leads to loss in $\Delta\Psi$ and release of cytochrome *c*, a necessary event in the mitochondrial cell death pathway (64, 65), from the mitochondrial intermembrane space into the cytosol. Following its release into the cytosol, the proapoptotic cytochrome *c* forms the apoptosome complex with apoptosis protease-activating factor-1 to induce caspases and subsequent apoptosis (66). We observed that ER stress leads to activation of PTP, loss in $\Delta\Psi$, and cytochrome *c* release from the mitochondria and that these events are amplified in OE INS-1 cells and are inhibited by inactivation of iPLA$_2\beta$. Furthermore, release of Smac is evident during ER stress and its accumulation in the cytosol is also amplified in OE INS-1 cells. The proapoptotic effects of Smac are thought to be due to its abilities to induce cytochrome *c* release (67) and to inhibit inhibitor of apoptosis proteins, thus promoting caspase activation cascade initiated by the release of cytochrome *c* (68). Our findings therefore support the possibility that iPLA$_2\beta$ contributes to activation of mitochondria-related apoptotic events. Consistent with this, we find that ER stress promotes accumulation of iPLA$_2\beta$, ceramide generation, and sphingomyelin hydrolysis in the ER (34) and mitochondrial fractions. Interestingly, ceramide generation and NSMase expression during ER stress are also amplified in iPLA$_2\beta$ overexpressing INS-1 cells and are inhibited by BEL (34). These findings indicate that iPLA$_2\beta$ activation during ER stress is a key modulator of subsequent disruption of mitochondrial membrane permeability and eventual apoptotic INS-1 cell death.

The effects of ER stress on PTP and $\Delta\Psi$ are mimicked in INS-1 cells exposed to a ceramide analog (C2-CM). This is not unexpected, as PTP activation, loss in $\Delta\Psi$, and overall mitochondrial dysfunction (52, 53) following ceramide accumulations or exposure to ceramide analogs are reported to occur in other cell types (69–71). Furthermore, elevations in cAMP have been demonstrated to suppress ceramide-induced cell death (55). We therefore compared the protective effects of increasing intracellular levels of cAMP in ceramide-treated and ER-stressed cells. We find that pretreatment of INS-1 cells with forskolin, an adenylate cyclase activator, suppresses both ceramide-induced apoptosis and loss in $\Delta\Psi$. Similarly, forskolin attenuates ER stress-induced $\Delta\Psi$ loss and apoptosis. These findings imply that pathways leading to apoptosis following exposure to ceramides or during ER stress converge downstream at the mitochondrial level.

Ceramides can be generated via multiple pathways and in contrast to contribution of the *de novo* pathway to lipoapoptosis of β-cells in ZDF rats (72) or of pancreatic islets exposed to free fatty acids (73, 74), ceramide accumulation in INS-1 cells during ER stress occurs predominantly via hydrolysis of sphingomyelins by neutral sphingomyelinase (34, 35). In support of this, ER stress neither induces serine palmitoyltransferase, which catalyzes the rate-limiting step in the *de novo* pathway, nor does inhibition of serine palmitoyltransferase suppress ER stress-induced apoptosis and ceramide generation (34). In con-

trast, neutral sphingomyelinase expression increases following induction of ER stress and inhibition of neutral sphingomyelinase with GW4869 or its knockdown using small interfering RNA suppresses sphingomyelin hydrolysis, ceramide generation, and apoptosis due to ER stress (34). To determine if a similar ceramide-generating mechanism is expressed and is activated in the ER or mitochondria during ER stress, ER and mitochondrial fractions were prepared from INS-1 cells and analyzed by ESI/MS/MS. Such analyses suggested that ER stress induces ceramide generation and sphingomyelin hydrolysis in both the ER and mitochondrial fractions of INS-1 cells. Although the ER and mitochondrial fractions were not completely free of plasma membrane contamination, it is not totally unexpected that both the ER and the mitochondria are capable of generating ceramides via sphingomyelin hydrolysis. The membranes of the nucleus and ER are contiguous (75, 76) and they both express NSMase (77, 78). Purified mitochondria from cells exposed to various agents have increased ceramide levels (53) and the contribution of mitochondrial sphingomyelin hydrolysis to ceramide generation and apoptosis has been demonstrated in other studies (79, 80). These observations suggesting that the ER and mitochondria express components of sphingolipid metabolism raise the possibility that these organelles may also contribute to the generation of ceramides via sphingomyelin hydrolysis during apoptosis.

Determination of the pooled mass of ceramide and sphingomyelin molecular species, relative to protein content (pmol/mg protein), reveal amplified ceramide generation and sphingomyelin hydrolysis in the ER and mitochondrial fractions of OE cells, relative to Vector cells, following induction of ER stress. The combined (ER + mitochondria) increase in ceramide and decrease in sphingomyelins, in the ER and mitochondrial fractions are found to be nearly 2-fold higher in the OE cells, relative to the Vector cells. Consistent with ceramide generation via sphingomyelins the magnitude of ceramide increase is similar to the magnitude of decrease in sphingomyelins in the ER and mitochondrial fractions of both Vector and OE INS-1 cells. The likelihood that ceramides generated via this pathway affect the mitochondria is supported by the finding that the NSMase inhibitor GW4689 suppresses both cytochrome *c* release and loss in $\Delta\Psi$. In agreement with this possibility, targeting of SMase to the mitochondria of MCF7 cells has been reported to cause cytochrome *c* release and apoptosis (80).

As summarized in the scheme in Fig. 11, we report here that induction of ER stress in INS-1 cells promotes expression of ER stress factors and events recognized to occur when the intrinsic apoptotic pathway is triggered. These include loss in mitochondrial membrane potential, activation of mitochondrial permeability transition pore, and release of cytochrome *c* and Smac from the mitochondria into the cytosol. All of these, being hallmarks of apoptosis, point to a mitochondrial involvement in ER stress-induced β-cell apoptosis. Because our findings indicate that these mitochondrial events are sensitive to iPLA$_2\beta$ activation and that iPLA$_2\beta$-mediated ceramide generation is integral to the apoptotic process, it is proposed that the iPLA$_2\beta$-ceramide axis plays a key role in the cross-talk between the ER and mitochondria and contributes to β-cell death due to ER stress. The specific mechanism by which ceramides can cause mitochondrial dysfunction remains to be answered (79) although interaction with proapoptotic factors Bak/Bax (81), increasing uptake of ER-derived Ca^{2+} into the mitochondria (82), and affecting mitochondrial electron transport chain components (52, 53) have been proposed to be involved. Alternatively, ceramides have been suggested to form channels in the outer mitochondrial membrane at concentrations that are consistent with mitochondrial ceramide levels in cells undergoing apoptotic cell death (45, 83).

REFERENCES

1. Tisch, R., and McDevitt, H. (1996) *Cell* **85,** 291–297
2. Mathis, D., Vence, L., and Benoist, C. (2001) *Nature* **414,** 792–798
3. DeFronzo, R. A. (1988) *Diabetes* **37,** 667–687
4. Kudva, Y. C., and Butler, P. C. (1997) in *Clinical Research in Diabetes and Obesity* (Draznin, B., and Rizza, R., eds) pp. 119–136, Humana Press, Totowa, NJ
5. Butler, A. E., Janson, J., Bonner-Weir, S., Ritzel, R., Rizza, R. A., and Butler, P. C. (2003) *Diabetes* **52,** 102–110
6. Yoon, K. H., Ko, S. H., Cho, J. H., Lee, J. M., Ahn, Y. B., Song, K. H., Yoo, S. J., Kang, M. I., Cha, B. Y., Lee, K. W., Son, H. Y., Kang, S. K., Kim, H. S., Lee, I. K., and Bonner-Weir, S. (2003) *J. Clin. Endocrinol. Metab.* **88,** 2300–2308
7. Kloppel, G., Lohr, M., Habich, K., Oberholzer, M., and Heitz, P. U. (1985) *Surv. Synth. Pathol. Res.* **4,** 110–125
8. Stefan, Y., Orci, L., Malaisse-Lagae, F., Perrelet, A., Patel, Y., and Unger, R. H. (1982) *Diabetes* **31,** 694–700
9. Bernard, C., Berthault, M.-F., Saulnier, C., and Ktorza, A. (1999) *Fed. Am. Soc. Exp. Biol. J.* **13,** 1195–1205
10. Pick, A., Clark, J., Kubstrup, C., Levisetti, M., Pugh, W., Bonner-Weir, S., and Polonsky, K. S. (1998) *Diabetes* **47,** 358–364
11. Butler, A. E., Janson, J., Soeller, W. C., and Butler, P. C. (2003) *Diabetes* **52,** 2304–2314
12. Araki, E., Oyadomari, S., and Mori, M. (2003) *Exp. Biol. Med.* **228,** 1213–1217
13. Cardozo, A. K., Ortis, F., Storling, J., Feng, Y.-M., Rasschaert, J., Tonnesen, M., Van Eylen, F., Mandrup-Poulsen, T., Herchuelz, A., and Eizirik, D. L. (2005) *Diabetes* **54,** 452–461
14. Diaz-Horta, O., Kamagate, A., Herchuelz, A., and Van Eylen, F. (2002) *Diabetes* **51,** 1815–1824
15. Rao, R. V., Castro-Obregon, S., Frankowski, H., Schuler, M., Stoka, V., del Rio, G., Bredesen, D. E., and Ellerby, H. M. (2002) *J. Biol. Chem.* **277,** 21836–21842
16. Kaufman, R. J. (1999) *Genes Dev.* **13,** 1211–1233
17. Oyadomari, S., Araki, E., and Mori, M. (2002) *Apoptosis* **7,** 335–345
18. Oyadomari, S., Koizumi, A., Takeda, K., Gotoh, T., Akira, S., Araki, E., and Mori, M. (2002) *J. Clin. Investig.* **109,** 525–532
19. Socha, L., Silva, D., Lesage, S., Goodnow, C., and Petrovsky, N. (2003) *Ann. N. Y. Acad. Sci.* **1005,** 178–183
20. Harding, H. P., Zeng, H., Zhang, Y., Jungries, R., Chung, P., Plesken, H., Sabatini, D. D., and Ron, D. (2001) *Cell Prog.* **7,** 1153–1163
21. Delepine, M., Nicolino, M., Barrett, T., Golamaully, M., Lathrop, G. M., and Julier, C. (2000) *Nat. Genet.* **25,** 406–409
22. Takeda, K., Inoue, H., Tanizawa, Y., Matsuzaki, Y., Oba, J., Watanabe, Y., Shinoda, K., and Oka, Y. (2001) *Hum. Mol. Genet.* **10,** 477–484
23. Fonseca, S. G., Fukuma, M., Lipson, K. L., Nguyen, L. X., Allen, J. R., Oka, Y., and Urano, F. (2005) *J. Biol. Chem.* **280,** 39609–39615
24. Oyadomari, S., Takeda, K., Takiguchi, M., Gotoh, T., Matsumoto, M., Wada, I., Akira, S., Araki, E., and Mori, M. (2001) *Proc. Natl. Acad. Sci.* **98,** 10845–10850
25. Kroncke, K.-D., Brenner, H.-H., Rodriguez, M.-L., Etzkorn, K., Noack, E. A., Kolb, H., and Kolb-Bachofen, V. (1993) *Biochim. Biophys. Acta* **1182,** 221–229
26. Corbett, J. A., and McDaniel, M. L. (1992) *Diabetes* **41,** 897–903
27. Mandrup-Poulsen, T. (1996) *Diabetologia* **39,** 1005–1029
28. Yamada, T., Ishihara, H., Tamura, A., Takahashi, R., Yamaguchi, S., Takei,

D., Tokita, A., Satake, C., Tashiro, F., Katagiri, H., Aburatani, H., Miyazaki, J.-i., and Oka, Y. (2006) *Hum. Mol. Genet.* **15,** 1600–1609
29. Ron, D. (2002) *J. Clin. Investig.* **110,** 1383–1388
30. Cohen, G. M. (1997) *Biochem. J.* **326,** 1–16
31. Duchen, M. R. (2000) *J. Physiol.* **529,** 57–68
32. Berridge, M. J. (2002) *Cell Calcium* **32,** 235–249
33. Nowatzke, W., Ramanadham, S., Ma, Z., Hsu, F. F., Bohrer, A., and Turk, J. (1998) *Endocrinology* **139,** 4073–4085
34. Lei, X., Zhang, S., Bohrer, A., Bao, S., Song, H., and Ramanadham, S. (2007) *Biochemistry* **46,** 10170–10185
35. Ramanadham, S., Hsu, F. F., Zhang, S., Jin, C., Bohrer, A., Song, H., Bao, S., Ma, Z., and Turk, J. (2004) *Biochemistry* **43,** 918–930
36. Gijon, M. A., and Leslie, C. C. (1997) *Semin. Cell Dev. Biol.* **8,** 297–303
37. Schaloske, R. H., and Dennis, E. A. (2006) *Biochim. Biophys. Acta* **176,** 1246–1259
38. Ma, Z., Ramanadham, S., Kempe, K., Chi, X. S., Ladenson, J., and Turk, J. (1997) *J. Biol. Chem.* **272,** 11118–11127
39. Turk, J., and Ramanadham, S. (2004) *Can. J. Physiol. Pharmacol.* **82,** 824–832
40. Wilkins, W. P., III, and Barbour, S. E. (2008) *Curr. Drug Targ.* **9,** 683–697
41. Ramanadham, S., Gross, R. W., Han, X., and Turk, J. (1993) *Biochemistry* **32,** 337–346
42. Ogretmen, B., and Hannun, Y. A. (2004) *Nat. Rev. Cancer* **4,** 604–616
43. van Blitterswijk, W. J., van der Luit, A. H., Veldman, R. J., Verheij, M., and Borst, J. (2003) *Biochem. J.* **369,** 199–211
44. Hajnoczky, G., Csordas, G., Madesh, M., and Pacher, P. (2000) *J. Physiol.* **529,** 69–81
45. Siskind, L. J., Kolesnick, R. N., and Colombini, M. (2006) *Mitochondrion* **6,** 118–125
46. Desagher, S., Osen-Sand, A., Nichols, A., Eskes, R., Montessuit, S., Lauper, S., Maundrell, K., Antonsson, B., and Martinou, J.-C. (1999) *J. Cell Biol.* **144,** 891–901
47. Predescu, S. A., Predescu, D. N., Knezevic, I., Klein, I. K., and Malik, A. B. (2007) *J. Biol. Chem.* **282,** 17166–17178
48. Ramanadham, S., Bohrer, A., Mueller, M., Jett, P., Gross, R. W., and Turk, J. (1993) *Biochemistry* **32,** 5339–5351
49. Ramanadham, S., Hsu, F.-F., Bohrer, A., Ma, Z., and Turk, J. (1999) *J. Biol. Chem.* **274,** 13915–13927
50. Hsu, F. F., and Turk, J. (2002) *J. Am. Soc. Mass Spectrom.* **13,** 558–570
51. Petronilli, V., Miotto, G., Canton, M., Brini, M., Colonna, R., Bernardi, P., and Di Lisa, F. (1999) *Biophys. J.* **76,** 725–734
52. Birbes, H., Luberto, C., Hsu, Y.-T., El Bawab, S., Hannun, Y. A., and Obeid, L. M. (2005) *Biochem. J.* **386,** 445–451
53. Dai, Q., Liu, J., Chen, J., Durrant, D., McIntyre, T. M., and Lee, R. M. (2004) *Oncogene* **23,** 3650–3658
54. Hsu, F. F., and Turk, J. (2000) *J. Am. Soc. Mass Spectrom.* **11,** 437–449
55. Rath, G. M., Schneider, C., Dedieu, S., Sartelet, H., Morjani, H., Martiny, L., and El Btaouri, H. (2006) *Int. J. Biochem. Cell Biol.* **38,** 2219–2228
56. Green, D. R., and Kroemer, G. (2004) *Science* **305,** 626–629
57. Groenendyk, J., and Michalak, M. (2005) *Acta Biochim. Pol.* **52,** 381–395
58. Chan, S. L., Fu, W., Zhang, P., Cheng, A., Lee, J., Kokame, K., and Mattson, M. P. (2004) *J. Biol. Chem.* **279,** 28733–28743
59. Ermak, G., and Davies, K. J. (2002) *Mol. Immunol.* **38,** 713–721
60. Shiraishi, H., Okamoto, H., Yoshimura, A., and Yoshida, H. (2006) *J. Cell Sci.* **119,** 3958–3966
61. Di Sano, F., Ferraro, E., Tufi, R., Achsel, T., Piacentini, M., and Cecconi, F. (2006) *J. Biol. Chem.* **281,** 2693–2700
62. Li, J., Lee, B., and Lee, A. S. (2006) *J. Biol. Chem.* **281,** 7260–7270
63. Chipuk, J. E., Bouchier-Hayes, L., and Green, D. R. (2006) *Cell Death Differ.* **13,** 1396–1402
64. Garrido, C., Galluzzi, L., Brunet, M., Puig, P. E., Didelot, C., and Kroemer, G. (2006) *Cell Death Differ.* **13,** 1423–1433
65. Korsmeyer, S. J., Wei, M. C., Saito, M., Weiler, S., Oh, K. J., and Schlesinger, P. H. (2000) *Cell Death Differ.* **7,** 1166–1173
66. Schafer, Z. T., and Kornbluth, S. (2006) *Dev. Cell* **10,** 549–561
67. Hasenjager, A., Gillissen, B., Muller, A., Normand, G., Hemmati, P. G., Schuler, M., Dorken, B., and Daniel, P. T. (2004) *Oncogene* **23,** 4523–4535
68. Wu, G., Chai, J., Suber, T. L., Wu, J.-W., Du, C., Wang, X., and Shi, Y. (2000) *Nature* **408,** 1008–1012
69. Falluel-Morel, A., Aubert, N., Vaudry, D., Basille, M., Fontaine, M., Fournier, A., Vaudry, H., and Gonzalez, B. J. (2004) *J. Neurochem.* **91,** 1231–1243
70. Kong, J., Klassen, S., and Rabkin, S. (2005) *Mol. Cell. Biochem.* **278,** 39–51
71. Muranaka, S., Kanno, T., Fujita, H., Kobuchi, H., Akiyama, J., Yasuda, T., and Utsumi, K. (2004) *Free Radic. Res.* **38,** 613–621
72. Shimabukuro, M., Higa, M., Zhou, Y.-T., Wang, M.-Y., Newgard, C. B., and Unger, R. H. (1998) *J. Biol. Chem.* **273,** 32487–32490
73. Kelpe, C. L., Moore, P. C., Parazzoli, S. D., Wicksteed, B., Rhodes, C. J., and Poitout, V. (2003) *J. Biol. Chem.* **278,** 30015–30021
74. Lupi, R., Dotta, F., Marselli, L., Del Guerra, S., Masini, M., Santangelo, C., Patane, G., Boggi, U., Piro, S., Anello, M., Bergamini, E., Mosca, F., Di Mario, U., Del Prato, S., and Marchetti, P. (2002) *Diabetes* **51,** 1437–1442
75. Holz, G. G., Leech, C. A., Heller, R. S., Castonguay, M., and Habener, J. F. (1999) *J. Biol. Chem.* **274,** 14147–14156
76. Schievella, A. R., Regier, M. K., Smith, W. L., and Lin, L.-L. (1995) *J. Biol. Chem.* **270,** 30749–30754
77. Fensome, A. C., Josephs, M., Katan, M., and Rodrigues-Lima, F. (2002) *Biochem. J.* **365,** 69–77
78. Tamiya-Koizumi, K., Umekawa, H., Yoshida, S., and Kojima, K. (1989) *J. Biochem.* (*Tokyo*) **106,** 593–598
79. Birbes, H., Bawab, S. E., Obeid, L. M., and Hannun, Y. A. (2002) *Adv. Enzymol. Reg.* **42,** 113–129
80. Birbes, H., El Bawab, S., Hannun, Y. A., and Obeid, L. M. (2001) *Fed. Am. Soc. Exp. Biol. J.* **15,** 2669–2679
81. Morales, M. C., Perez-Yarza, G., Rementeria, N. N., Boyano, M. D., Apraiz, A., Gomez-Munoz, A., Perez-Andres, E., and Asumendi, A. (2007) *Free Radic. Res.* **41,** 591–601
82. Darios, F., Lambeng, N., Troadec, J. D., Michel, P. P., and Ruberg, M. (2003) *J. Neurochem.* **84,** 643–654
83. Siskind, L. (2005) *J. Bioenerg. Biomemb.* **37,** 143–153